CHAPTER 2

VALIDATION OF RAIN RATE ESTIMATION IN HURRICANES FROM THE STEPPED FRQUENCY MICROWAVE RADIOMETER (SFMR) — ALGORITHM CORRECTION AND ERROR ANALYSIS

2.1 Abstract

Simultaneous observations by the Lower Fuselage (LF) radar, the tail (TA) radar, and the Stepped Frequency Microwave Radiometer (SFMR) on board the National Oceanic and Atmospheric Administration (NOAA) WP-3D aircraft are used to validate the rainfall rate estimates from microwave emission measurements of SFMR in tropical cyclones. Data collected in Hurricane Bonnie (1998) and Hurricane Humberto (2001) with a total of 820 paired samples are used in the comparisons. The SFMR 10-s path-integrated rain rates are found to be insensitive, with an overestimate in light rain and an underestimate in heavy rain relative to radar rainfall estimates. Examination of the existing SFMR algorithm shows that the coefficient should be changed in the attenuation — rain rate relationship used in the inversion algorithm. After this correction, a linear regression result with a correlation coefficient of 0.8 and a slope close to 1 is obtained. But an overall high bias of 5 mm/hr of the SFMR rainfall estimate relative to radar is also found. The error analysis shows that the bias is nearly independent of rain type, a result confirming Jorgensen and Willis's (1982) conclusion that the drop size distributions

between convective and stratiform rain in hurricanes are similar. It is also shown that the bias is a weak function of wind speed, as well as a weak inverse function of the radial distance to the hurricane center. We are able to rule out temperature dependence as the main explanation. We speculate that the bias results from a combination of two factors: sensitivity of SFMR estimates to fractional coverage of the sea surface to foam and spray, or a result of a downward increase of radar reflectivity in the high wind regions. If the true downward increase is 1-2 dBZ/km (c.f. Ferreira et al. 2001), the different elevations of the data from the TA radar and SFMR could account for up to 3-5 mm/hr bias.

2.2 Introduction

Accurate quantitative precipitation estimates within tropical cyclones over ocean is a challenging problem. Obviously, no surface rain gauge data are available. Research aircraft can fly through the storm and provide precipitation estimates from passive and active microwave instruments. This work describes the validation of path-integrated rain rates from the National Oceanic and Atmospheric Administration (NOAA) Hurricane Research Division's (HRD) Stepped-Frequency Microwave Radiometer (SFMR). The SFMR is designed for the measurement of sea surface wind speed and path-integrated rain rate. On board the NOAA WP-3D hurricane research aircraft, SFMR data are obtained on tropical cyclones over Atlantic Ocean during the NOAA HRD's annual program of research flights since 1980. Since 1999, the HRD began to transmit the real-time SFMR surface winds and rainfall rates to the National Hurricane Center (NHC) for application to hurricane forecasts. The advantage of SFMR is that it can potentially provide along aircraft track mapping of rain rates and surface wind speeds in high

temporal resolution (1 Hz). The SFMR-derived surface wind is one of the most important data sources of direct hurricane inner-core surface wind speed estimates available for NHC forecasters (Black et al. 2000). The SFMR surface wind estimates have been well validated by Global Positioning System (GPS) dropwindsonde measurements (Uhlhorn and Black 2003; Black et al. 2000) and have been universally accepted. It is very important for hurricane forecasters to get the real-time, relatively accurate rain rate data matched with the surface wind speed data. In this dissertation, SFMR rain rates are compared with airborne radar data from two independent hurricane cases.

It has been long known that microwave attenuation/extinction K (same as β_e given by (1.1)) by rainfall is strongly correlated with rain rate R (Ryde 1947; Wexler and Atlas 1963; Olsen et al. 1978). In SFMR frequencies (4.55-7.22 GHz), the radiative interaction with raindrops is in Rayleigh regime (rain particle sizes are smaller than the wavelengths, Pettey 2004). As discussed in section 1.2.2, in Rayleigh approximation, the extinction cross section $\sigma_e (\approx \sigma_a)$ is proportional to D^3, therefore K is proportional to D^3 according to (1.1). The rain rate R is proportional to $V(D)D^3$ according to (1.18), where the terminal fall speed $V(D)$ is approximately proportional to $D^{0.5}$ to D^1 for raindrops (Rodgers and Yau 1989). In fact, a specific K-R relationship depends on the frequency, raindrop size distribution (DSD), and temperature (Olsen et al. 1978). As more and more understanding on the K-R relationship was achieved, the SFMR rain algorithm was improved step by step. The first experimental SFMR rain rate measurements were made in Hurricane Allen in 1980 by the first SFMR instrument built by the National Aeronautics and Space Administration's (NASA) Langley Research Center in 1978 (Harrington 1980). Four selectable frequencies between 4.5 and 7.2 GHz were used to

produce a “stepping” procedure allowed for estimating the rain rate and wind speed. The first SFMR rainfall algorithm applied in Hurricane Allen (1980) data was developed and reported by Jones et al. (1981). By neglecting the effect of absorption by oxygen molecules, water vapor and nonprecipitation liquid water, the radiative transfer equation was solved to get the rain opacity τ , which can be related to K and the depth of the rain column h by:

$$\tau = \exp(-Kh) \tag{2.1}$$

neglecting the effect of scattering at SFMR frequencies. τ was further related to rain rate R by a linear relationship at a frequency of 6.6 GHz:

$$R = 320\tau \tag{2.2}$$

The value 320 was chosen empirically by data fitting. It could largely vary for different DSDs. Agreement between airborne radar and SFMR estimates for a pass of Hurricane Allen was found to be within a factor of 2. Black and Swift (1984) refined the SFMR rain algorithm by further solving the attenuation coefficient K from τ. Using brightness temperature measurements from two frequencies, K can be calculated iteratively. Applying a rain rate and frequency dependent power relationship between K and R derived by Olsen et al. (1978), SFMR rain rate was retrieved in a relatively good agreement with radar measurements. Despite the preliminary success in Allen, this original instrument was never again flown into a hurricane.

A new retrieval algorithm was implemented by Tanner et al. (1987; please see Uhlhorn and Black 2003 for the details) with the advent of a second SFMR designed and

built in 1982 (Swift et al. 1986). With 6 frequencies instead of 4 between 4.5 and 7.2 GHz used in the new SFMR, an inversion technique was developed to infer two parameters (wind speed and rain rate) from six brightness temperature measurements. The second SFMR was also improved in hardware in the following decade by setting up a new antenna, upgrading the receiver so that an improved spatial resolution and a stable calibration are gained. Since 1980, the SFMR has flown on 95 flights in 30 tropical cyclones (Uhlhorn and Black 2003).

The airborne radar has proven its ability in estimating rainfall in hurricanes. Jorgensen and Willis (1982) derived an overall Z-R relationship from three mature hurricanes by using airborne disdrometer observations and argued that this relationship could be used in both stratiform and convective rain regions of tropical cyclones without obvious bias. Marks (1985) has investigated the evolution of precipitation structure of Hurricane Allen (1980) by using airborne radar rainfall estimation. In this study, the SFMR rain rate measurements in tropical cyclones are evaluated against airborne radar data. The radar data used here are from the Lower Fuselage (LF) radar and the tail (TA) radar on the NOAA WP-3D aircraft.

The meaningfulness of validation is dependent on the quality of the validation data. The task of accurately quantifying radar-rainfall has proven to be difficult. The reasons are threefold: 1) Despite Jorgensen and Willis's (1982) result, the Z-R relationship depends on the raindrop size distribution that may vary from storm to storm or even from one part of a storm to another (Smith et al. 2001); 2) The LF radar has a beamfilling problem (see section 1.2.4 for definition) because of its large beam width (Amayenc et al. 1993; Baeck and Smith 1998; Durden et al. 1998); 3) The radar calibration could be a

problem (Klazura et al. 1999). Based on this understanding, we carefully chose two mature hurricane cases (Bonnie 1998 and Humberto 2001) so that Jorgensen and Willis's (1982) overall Z-R relationship can be approximately applied assuming that the DSD variation in mature hurricanes is not very large. A near optimal comparing scheme is used to assure that no inadequate beamfilling signal will be chosen from LF radar, which has a large vertical beam width ($4.1°$). The effect of different sample volumes among these three instruments, which are different by several orders of magnitude, is believed to be minimized by data averaging and interpolating procedures. This scheme also minimizes the attenuation effect and bright band contamination. It is well-known that LF and TA radars have suffered from calibration problems for years. Marks et al. (1993) found an 8.2 dBZ calibration error for the LF radar during Hurricane Anita (1977). In this study, reflectivity measurements from a well-calibrated radar (ER-2 Doppler radar) are used to estimate the offsets of LF and TA radar reflectivity (see appendix).

The purpose of this work is 1) to establish a relatively accurate radar rain rate dataset collocated with SFMR observations to validate SFMR retrieval; 2) to refine the existing SFMR rain algorithm to improve its performance; 3) to quantitatively demonstrate that the rainfall estimated by SFMR now has the capability of serving as an important operational tool for mapping the distribution of precipitation in hurricanes; 4) to quantitatively describe the SFMR rain error in convective and stratiform precipitation, its dependence on tropical storm parameters of interest, and direct possible future work based on the error analysis.

2.3 Data Sources and Processing

2.3.1 SFMR Data

The HRD SFMR measures the microwave emissions from sea surface and intervening precipitation at six frequencies (4.55, 5.06, 5.64, 6.34, 6.96, 7.22 GHz) from its along-track nadir view. Since the antenna main beamwidth ranges from $22°$ to $32°$, brightness temperatures at the six C-band channels can be obtained within footprints of 600~800 m depending upon the channel at a typical flight altitude of 1500 m (footprints would be larger if the flight altitude is higher). The hardware averaging time is set at 0.7 s, suggesting the theoretical single-measurement brightness temperature T_b resolution (noise) of ΔT_b = 0.4 K (Uhlhorn and Black 2003). The response time of the instrument is 0.85 s per channel. The time between completely independent sets of measurements is generally defined as twice the response, so the actual independent sampling time is 2×6 channels $\times$ 0.85 s per channel = 10 s (Uhlhorn and Black 2003).

Since rain is weakly attenuating at these microwave frequencies and the attenuation by rain is a function of electromagnetic wavelength, the frequency-stepping ability of the instrument suggests a procedure for retrieving the rain rate. Because the small ratio of raindrop diameter (< 6 mm) to the SFMR wavelength (~ 5 cm), the radiative interatcion is in the Rayleigh limit. As we see from (1.15) and (1.16), in the Rayleigh regime the absorption cross section is proportional to r^3, while the scattering cross section is proportional to r^6. Therefore for small raindrops, the scattering effect can be neglected. The SFMR algorithm is emission-based as mentioned above in section 1.2.2. A forward radiative transfer model was built by previous studies (Uhlhorn and Black 2003, Jones et al. 1981, Black and Swift 1984) by approximating the entire emission/absorption process

of rain. Given a physical model that relates attenuation coefficient K to measurements of T_b at several frequencies and a relationship between rain rate R and K, a set of simultaneous equations may be inverted to calculate the rain rate under practically all weather conditions. (See the appendices of Uhlhorn and Black 2003 for a detailed SFMR configuration and SFMR algorithm.)

A theoretical noise level of SFMR single-measurement T_b is about 0.4 K (Uhlhorn and Black 2003). For a rain rate less than 5 mm/hr, the sensitivity of changes in the T_b to changes in rain rate at SFMR frequencies and nadir incidence angle is so weak that it is lost to its noise, and a solution is normally not possible. The minimum retrievable surface wind speed is 10 m/s. The SFMR algorithm is suitable only for measurements over ocean. It recognizes measurements entirely over land by a T_b threshold of 280 K. But when the antenna beam is partially filled by land, false rain rate retrieval can occur. In this comparison, rain rates < 5 mm/hr or measurements within 10 km of land are not included.

The algorithm outputs a rain rate estimate from the set of SFMR T_b measured at a rate of 1 Hz, but truly independent measurements are possible only at a slower sampling rate of 0.1 Hz, corresponding to a 10-s temporal resolution. For comparison with the airborne radar rain rate, a 10-s average SFMR value is calculated. Each of the independent variables (time and location) is adjusted to correspond to the averaged rain rate value.

2.3.2 TA Radar Data

The tail (TA) radar installed on the WP-3D N43RF aircraft is a vertical scanning X-band (3.22 cm) radar with Doppler capability. It has a vertical beamwidth of $1.9°$ and a horizontal beamwidth of $1.35°$. The spatial resolution along any radial ray is 75 m. The antenna, located in the tail of the aircraft, sweeps through the azimuth angles of $0° - 360°$ at an elevation angle of $\pm 20^{\circ}$ relative to the plane perpendicular to the aircraft ground track. Thus, the whole storm can be sampled by those vertical sweeps along the aircraft track, typically each 6-s at an aircraft ground speed of 100-120 m/s.

The X-band radar is strongly affected by attenuation from intervening precipitation particles. For minimizing the effect of attenuation, Marks (1985) constructed vertical time cross sections along the flight track and used only the radials pointing above and below the radar. In this comparison, only vertical cross section data from TA radar are included. Based on the vertical cross section image of TA reflectivity, rain type (stratiform/convective) is separated subjectively according to bright band and local reflectivity gradient and maximum (Steiner et al. 1995).

Furthermore, during some hurricane seasons including 1998 and 2001, the French dual-beam antenna system was mounted on the N43RF TA radar. This antenna system carries two antennae, one pointing $20°$ forward and one pointing $20°$ aft. In the research fore-aft scanning mode, the radar transmitter has to switch from one antenna to the other after every sweep. The problem is that during this switch, the transmitter needs to be shut off for a few microseconds. The procedure usually affects the data quality for around nadir looking rays. In investigating the Bonnie and Humberto cases, we found that in the vertical time cross section constructed by using only the rays pointing above or below

radar, the reflectivity is not continuous. Usually, the reflectivity values below the radar are much smaller those above radar. This problem is probably a result of the transmitter switching. Therefore, we used the averaged radar reflectivity between the first bin above the aircraft altitude (typically 1.5~2 km) and the bin at 3 km height toward the zenith to compare with SFMR along-track measurements. This averaged radar reflectivity has 6-s temporal resolution along the aircraft track. It is further interpolated into 10-s resolution by a "nearest neighbor" method and converted into rain rate by using Jorgensen and Willis (1982)'s overall Z-R relationship:

$$Z = 300R^{1.35} \tag{2.3}$$

where Z is in mm^6/m^3, R is in mm/hr. This comparison is based on an assumption that in the hurricane precipitation environment, the vertical rain rate profile doesn't change too much between the surface and 3 km above sea level. The error caused by this assumption will be discussed later.

2.3.3 LF Radar Data

The WP-3D C-band (5.59cm) Lower Fuselage (LF) radar scans horizontally with a radial spatial resolution of 750 m. It has a vertical beamwidth of 4.1° and horizontal beamwidth of 1.1° (see the appendix of Jorgensen 1984a for detail). Its purpose is to provide the plain view of the radar structure of tropical cyclones. A single sweep of the LF radar takes about 30-s. But the major problems of LF radar are 1) sea clutter contamination, 2) nonuniform beamfilling, and 3) attenuation by intervening precipitation. The first two problems are mainly produced by the wide vertical

beamwidth and antenna side lobes. Usually, the sea clutter problem could be minimized by lifting the elevation angle during radar operation. Marks (1985) gave a quantitative estimation of the mean signal loss caused by the nonuniform beamfilling problem of the LF. They showed that at an altitude of 1500 m, the mean loss is about 5 dB at the range of 100 km from radar, and increases up to 30 dB at the range of 300 km from radar. They also showed that typical losses as a result of rain attenuation for a wavelength of 5.5 cm are about half those caused by the nonuniform beamfilling problem. They developed a technique to minimize these two effects by mapping time composites rather than a single sweep.

For comparing with SFMR along-track measurements, the LF data used here is from averaging the reflectivities into of $\pm 5°$ around the direction of the flight track at a range of 7 km away from the airplane. Therefore we get one mean reflectivity value for a single sweep, with a temporal resolution of about 30-s since the antenna rotates twice a minute. We choose data at 7 km away from radar because 1) it is close enough to the radar so that the sea clutter, the nonuniform beamfilling, and attenuation problems will be negligible in most cases; 2) it is far away enough from radar to avoid the first several bins from the radar which are contaminated; 3) at the usual elevation angle of $3° - 4°$, at 7 km range, the beam is about 0.4 km above the radar altitude, a level of about 2~2.5 km above sea level. This averaged LF reflectivity at 2~2.5 km altitude is interpolated into 10-s temporal resolution and converted into rain rate value by using (2.3) similarly as what has been done for TA data. The LF data mapping is comparable with the scheme for TA data (section 2.3.2), assuring no bright band contamination.

2.4 Comparison of Results and Algorithm Correction

A total of 820 paired samples of SFMR and airborne radar rain rates were obtained from Hurricane Bonnie and Humberto on Aug. 24 and 26, 1998 and on Sept. 23 and 24, 2001 respectively (see Table 2.1 for a detailed summary of flights). The flight altitudes ranged from 1.5 to 2.1 km and each of the 4 flights sampled mature hurricanes with SFMR maximum wind above 34 m/s. To be included, the measurements had to be in a rain region based on the TA radar vertical cross section image. A minimum rain rate of 5 mm/hr was thresholded for both SFMR and radar observations. The geographic locations of SFMR/radar collocated rain rate measurements are plotted in Fig. 2.1 including flight tracks and storm centers during the time period of paired samples. All of the four flights included storm inner core region sampling. The classification of rain type has been done subjectively by examining the TA vertical cross section of reflectivity. A total of 563 (69%) paired samples were classified as stratiform; while 257 (31%) samples as convective. This classification has more convective points than the climatological average in hurricanes (Cecil et al, 2002). This over-sampling of heavy rain regions in the 820 data samples is an expected result because of our eliminating rain rates less than 5 mm/hr.

2.4.1 Regression Analysis

The scatterplots of SFMR versus LF and TA rain rates for all 820 paired samples are shown in Fig. 2.2. A high correlation between SFMR and radar measurements is shown by the correlation coefficients of 0.82 for SFMR relative to both LF and TA. But the slopes of the least squares best fits of 0.60 (SFMR versus LF) and 0.65 (SFMR versus

Table 2.1. Characteristics of Hurricane Bonnie and Humberto flights

Flight	Time (UTC)	Storm	Altitude (km)	Number of paired samples	Percentage of paired samples classified as stratiform	Percentage of paired samples classified as convective	SFMR wind maxim-um (m/s)
980824-I1	19:58-25:29	Bonnie	1.5	475	74% (353)	26% (122)	46
980826-I1	18:00-23:10	Bonnie	2.1	85	66% (56)	34% (29)	42
010923-I1	20:03-24:00	Humberto	1.8	110	52% (57)	48% (53)	43
010924-I1	20:52-25:01	Humberto	1.8	150	65% (97)	35% (53)	34

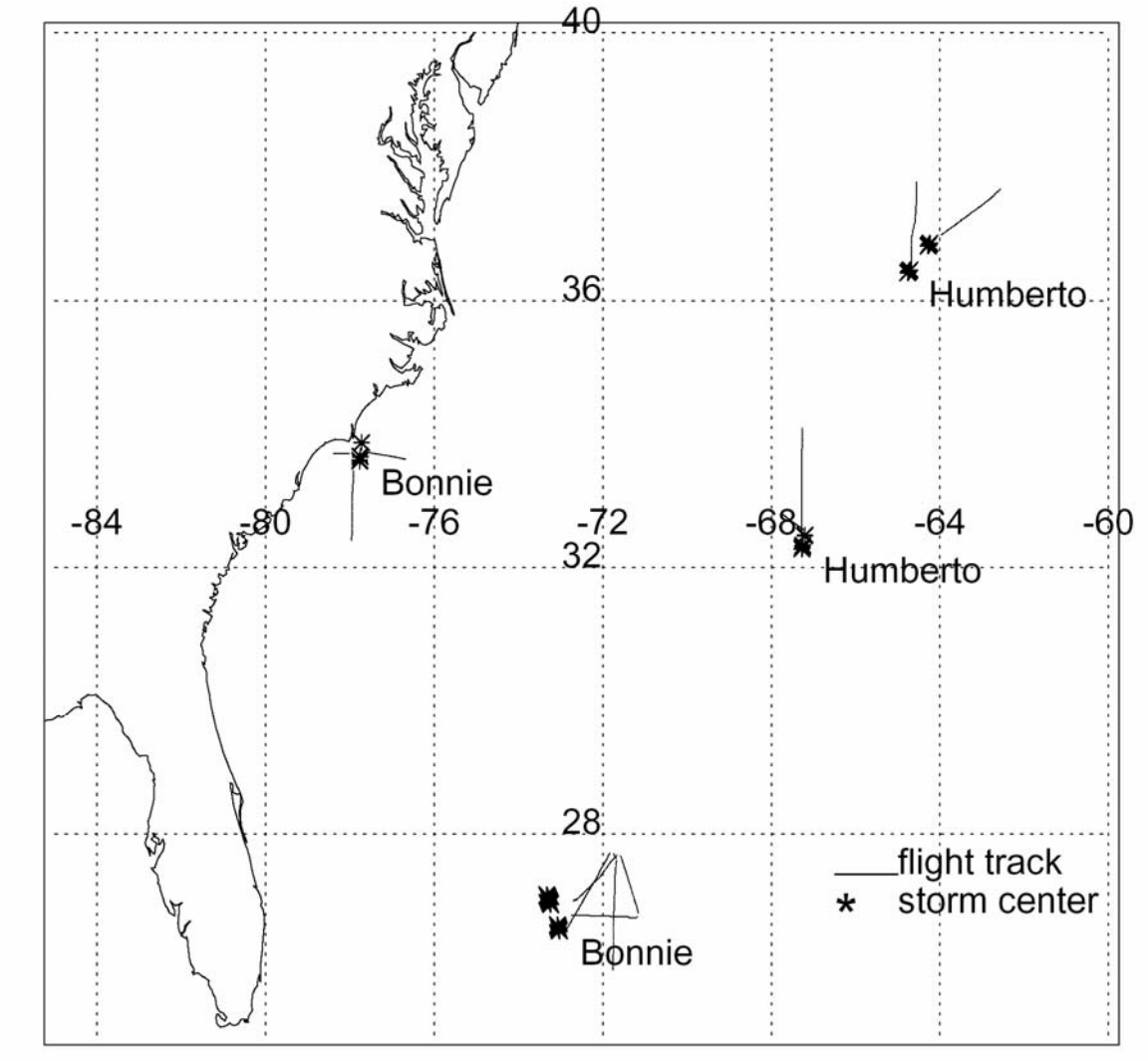

Figure 2.1. Geographic locations of SFMR/radar co-located rain rate measurements used in this study. Flight tracks are indicated by solid line and storm centers during the time period of paired samples are indicated by (*). Storm names related to each flight are printed in the figure.

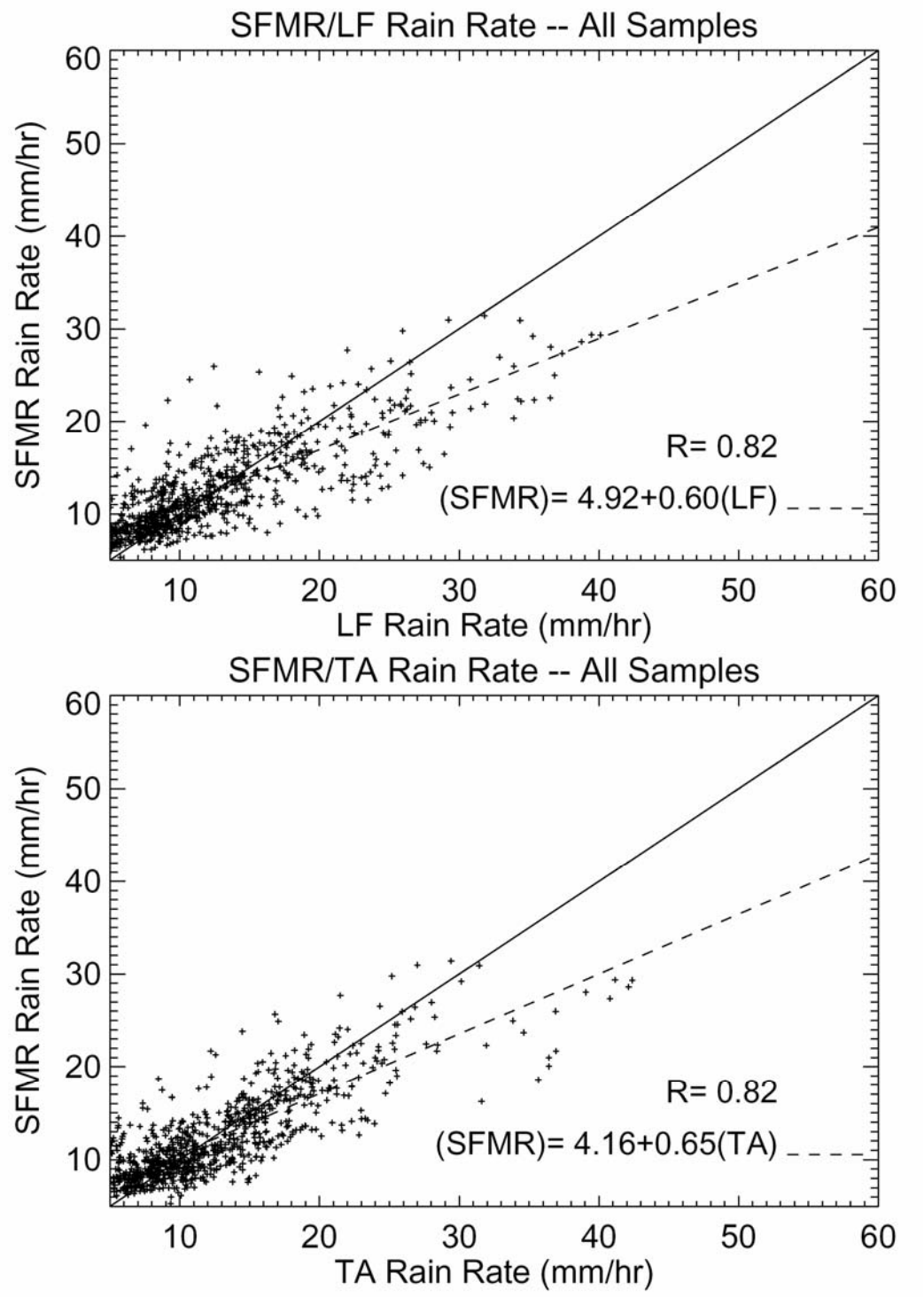

Figure 2.2. SFMR-LF and SFMR-TA rain rate comparisons for all samples. The solid line indicates perfect correlation and the dashed line indicates the best fit. Correlation coefficients are indicated.

TA) represent a severe insensitivity of SFMR rain retrievals with an overestimate for rain less than 10 mm/hr and an underestimate for rain greater than 10 mm/hr. This result is from the comparison with two independent sets of radar measurements. For independent storm cases and different rain types, the same tendency can be seen from the regression results. Table 2.2 gives the comparison of correlation coefficients and best fit equations of SFMR versus LF and TA rain rates for all samples, Bonnie only, Humberto only, stratiform only, and convective only. Although a small range of variation among those fitting parameters of subsets of samples, the systematic insensitivity of SFMR rain is obvious. The slope of best fit ranges from 0.54 to 0.68, while the intercept ranges from 3.73 to 6.88 mm/hr. Generally the regression equations have greater slope and smaller intercept between SFMR and TA than those between SFMR and LF. This better agreement of the SFMR rain with the TA radar will be discussed later.

2.4.2 Algorithm Correction

As described in Appendix A (b) of Uhlhorn and Black (2003), the SFMR rain algorithm used the following empirical relationship between rainfall attenuation coefficient K and rain rate R:

$$K = aR^b \tag{2.4}$$

where K is in Np/km (1 Np = 4.34 dB), R is in mm/hr; a and b are empirical parameters, depending on the DSD. Olsen et al. (1987) have shown that a is a function of R and frequency f:

$$a = gf^{n(R)} \tag{2.5}$$

Table 2.2. Correlation coefficients and best fit equations for different sample sets from least square regressions between SFMR and radar rain rates.

	SFMR vs. LF		SFMR vs. TA	
	Correlation coefficient	Best fit equation	Correlation coefficient	Best fit equation
All samples (820 samples)	0.82	SFMR= 4.92+0.6(LF)	0.82	SFMR= 4.16+0.65(TA)
Bonnie (560 samples)	0.81	SFMR= 5.11+0.54(LF)	0.82	SFMR= 3.83+0.65(TA)
Humberto (260 samples)	0.84	SFMR= 5.68+0.63(LF)	0.81	SFMR= 5.07+0.62(TA)
Stratiform (563 samples)	0.77	SFMR= 4.75+0.58(LF)	0.77	SFMR= 3.73+0.68(TA)
Convective (257 samples)	0.79	SFMR= 6.88+0.54(LF)	0.77	SFMR= 5.40+0.59(TA)

It has been shown that $n \approx 2.6R^{0.0736}$ (Atlas and Ulbrich, 1977) and $g = 1.87 \times 10^{-6}$ Np/km (Black and Swift, 1984). In the SFMR algorithm used here, the exponent b was taken to be 1.35 according to Jorgensen and Willis (1982). *In fact, b = 1.35 is for the radar reflectivity Z-R instead of K-R relationship in hurricanes.* As given by Willis and Jorgensen (1981) from aircraft microphysics observations of three mature hurricanes, the empirical relation derived between C-band radar reflectivity factor Z and attenuation coefficient K is:

$$K = 9.78 \times 10^{-6} Z^{0.85} \text{ (dB/km)} \qquad (2.6)$$

Combining (2.3) and (2.6), we get the exponent of K-R relation $b = 1.35 \times 0.85 = 1.15$.

A plot similar as Fig. A3 of Uhlhorn and Black (2003) but with a new value of exponent b =1.15 is given in Fig. 2.3, showing the rainfall attenuation coefficient K as a function of rain rate. This new parameter of b brings a big change in the SFMR rain retrieval. Table 2.3 lists the comparison of original SFMR retrieved and b-coefficient corrected SFMR rain rates at a set of K values at the highest frequency (7.22 GHz) of SFMR. Typically, the differences between original and corrected rain rates increase with rain intensity, reflecting a decreasing of b coefficient in Eq. (2.6). For example, an original retrieved rain rate of 5 mm/hr corresponds to a corrected one of 6.13 mm/hr, which is the new minimum retrievable rain rate value of SFMR; while an original retrieved 50 mm/hr corresponds to a corrected 80 mm/hr. This correction directly addresses the insensitivity problem of the SFMR old rainfall algorithm discussed in section 2.4.1.

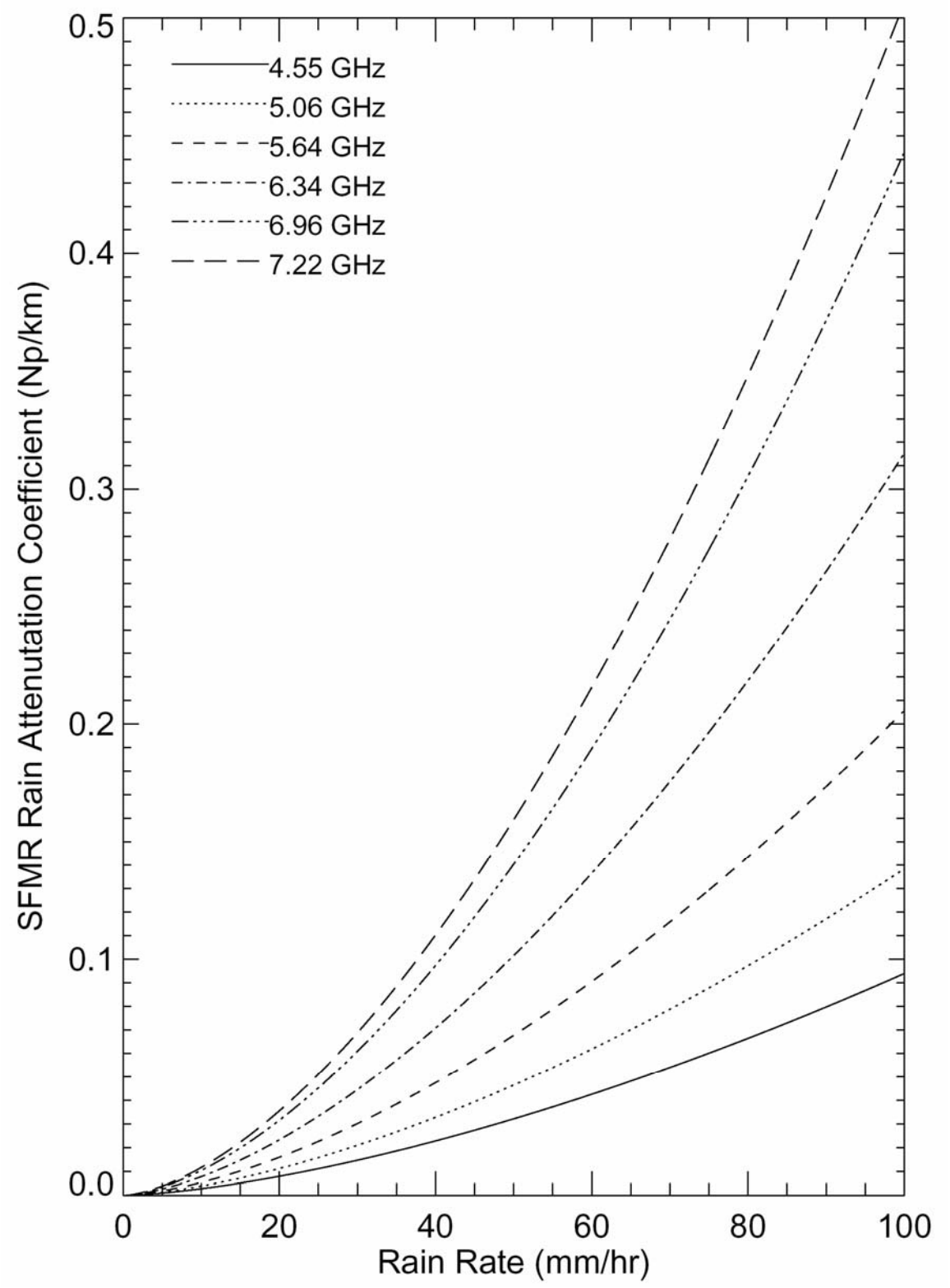

Figure 2.3. Rainfall attenuation coefficient K (Np/km) plotted as a function of rain rate (mm/hr) with the new exponent b=1.15 (see text for detail).

Table 2.3. Comparison of original SFMR retrieved and b-coefficient corrected SFMR rain rates at a set of K values at the highest frequency (7.22 GHz) of SFMR.

K at 7.22 GHz (Np/km)	0.00388	0.01165	0.03555	0.06881	0.11033	0.15946	0.21573
Original SFMR rain rate (mm/hr)	5.00	10.00	20.00	30.00	40.00	50.00	60.00
Corrected SFMR rain rate (mm/hr)	6.13	13.33	28.90	45.38	62.48	80.03	97.95

After rerunning the SFMR retrieval program for the whole two storms dataset by adding a b-coefficient correction, the new linear regression result for all samples is given in Fig. 2.4. Although it sounds reasonable to set a new threshold of 6.13 mm/hr for both radar and SFMR data, we did not do that since it does not make any difference on the regression results. As expected, the SFMR rain rate is no longer insensitive compared with radar measurements. The new slope of least squares fit to the data is close to 1 for both SFMR versus LF and SFMR versus TA. The correlation coefficient remains unchanged, but generally, the SFMR rain rate is overestimated relative to radar measurement at a magnitude of 5 mm/hr as indicated by the mean error. The overestimation is nearly independent of magnitude. Similarly as in Table 2.2, Table 2.4 shows mean errors and least square best fit equations of corrected SFMR versus LF and TA rain rates for different storms and different rain types. Correlation coefficients are not listed because they are as same as those in Table 2.2. Again, no important difference is found. However, SFMR versus LF regressions still represent a greater disagreement, with slopes down to 0.85, intercept up to 8.33, and mean bias high up to 6.91.

The PDFs and CDFs of the distribution of errors, defined as SFMR minus LF and SFMR minus TA, are plotted in Fig. 2.5. Both PDFs peak at a positive value of 3~5 mm/hr, revealing an overestimation of SFMR. The CDFs indicate that the middle 50% of the errors range between approximately 0 and + 6 mm/hr.

Now it is time to explain in detail about the difference between TA and LF rain rate estimates comparing with SFMR. As noticed above, from Table 2.2, 2.4 and Fig. 2.2, 2.4, 2.5, an obvious difference exists between SFMR versus TA and SFMR versus LF, although the tendency remains similar. In general, the mean errors between SFMR

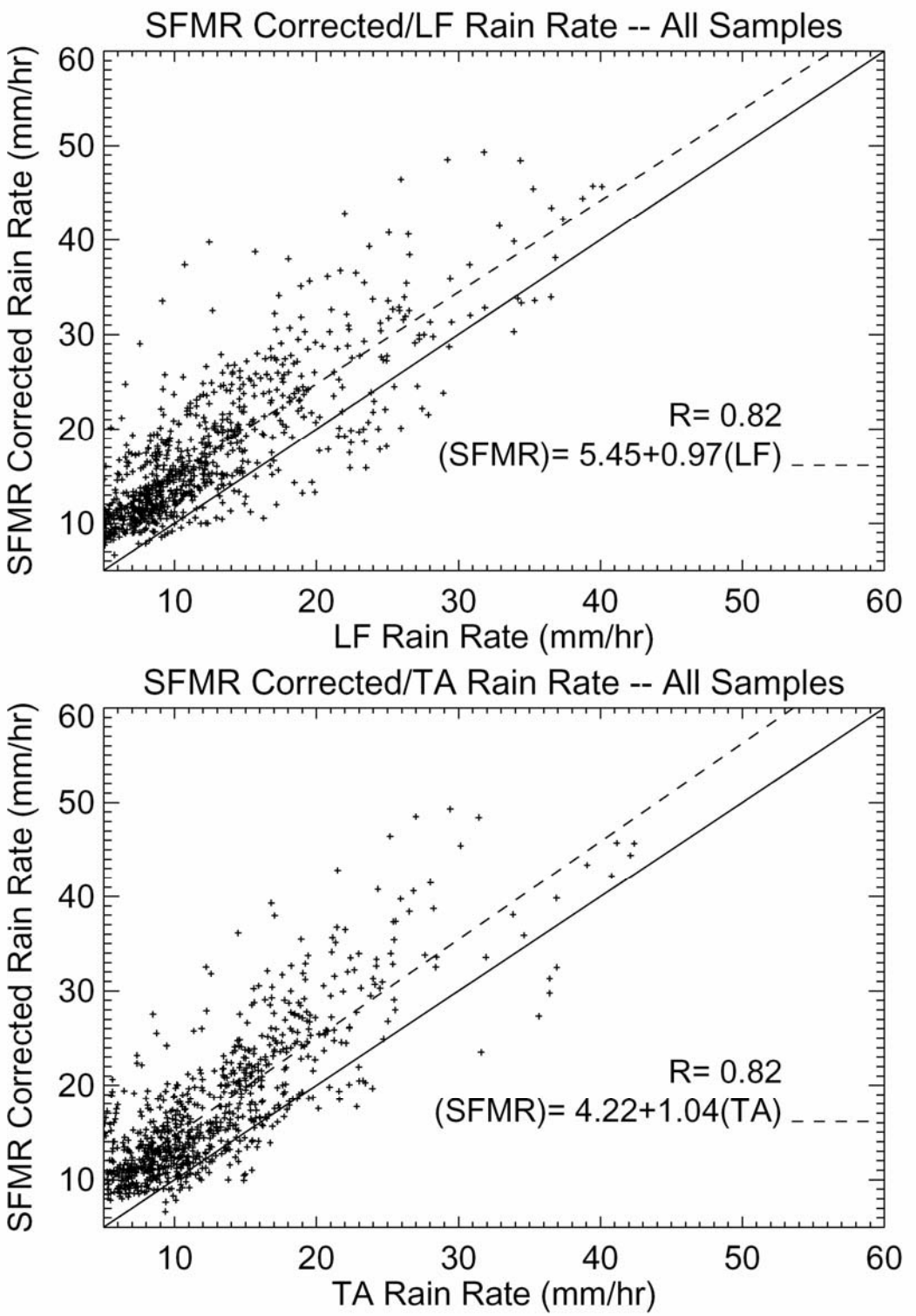

Figure 2.4. SFMR-LF and SFMR-TA rain rate comparisons for all samples after SFMR algorithm correction. The solid line indicates perfect correlation and the dashed line indicates the best fit. Mean rain rates (mm/hr) and correlation coefficients are indicated.

Table 2.4. Mean errors and best fit equations for different sample sets from least square regressions between SFMR corrected rain rates and radar rain rates (correlation coefficients are as same as in Table 2.2)

	SFMR vs. LF		SFMR vs. TA	
	Mean Error (mm/hr)	Best fit equation	Mean Error (mm/hr)	Best fit equation
All samples (820 samples)	5.05	SFMR=5.45+0.97(LF)	4.74	SFMR=4.22+1.04(TA)
Bonnie (560 samples)	4.18	SFMR=5.93+0.85(LF)	4.31	SFMR=3.92+1.03(TA)
Humberto (260 samples)	6.91	SFMR=6.54+1.03(LF)	5.67	SFMR=5.54+1.01(TA)
Stratiform (563 samples)	4.45	SFMR=5.37+0.91(LF)	4.47	SFMR=3.75+1.07(TA)
Convective (257 samples)	6.34	SFMR=8.33+0.88(LF)	5.32	SFMR=5.89+0.97(TA)

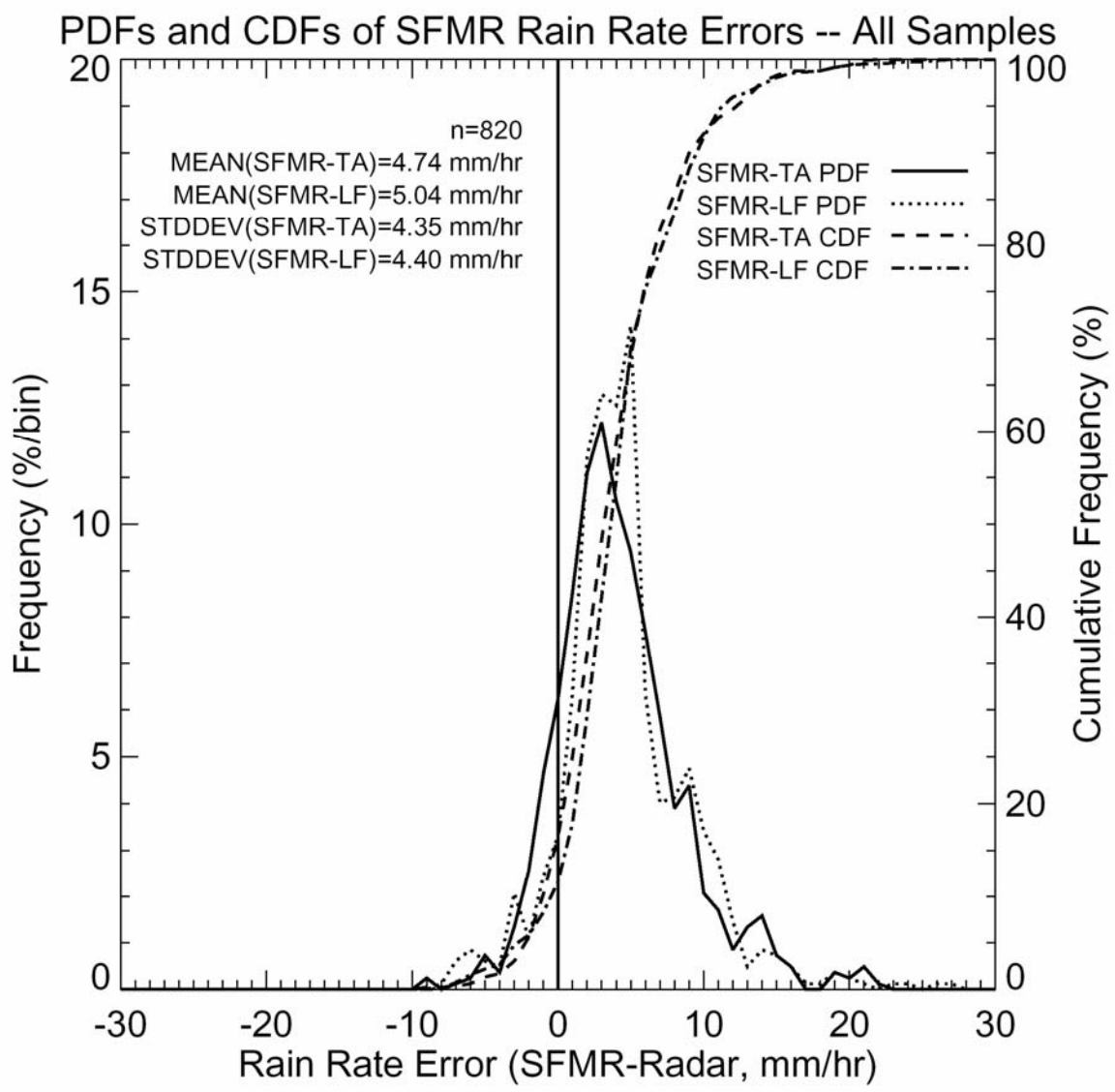

Figure 2.5. Probability density functions (PDF) of SFMR rain rate errors relative to TA rain rate (solid line), PDF of SFMR rain rate errors relative to LF rain rate (dot line), cumulative density function (CDF) of the SFMR rain rate errors relative to TA rain rate (dash line) and CDF of SFMR rain rate errors relative to LF rain rate (dash dot line) for all samples. For the n=820 observations, mean errors and standard deviations are indicated in the upper left corner of the figure.

and TA are less than those between SFMR and LF, and the slopes of best fit for SFMR versus TA are closer to 1 for both “all” samples and four subsamples (Table 2.4), although correlation coefficients remain similar for both comparisons (Table 2.2). From the CDFs of SFMR errors (Fig. 2.5), for most percentiles, SFMR minus LF is larger than SFMR minus TA by about 0.2~0.4 mm/hr. This is also indicated by mean errors shown in Fig. 2.5. The systematic difference is not surprising if we consider the different data processing scheme for three instruments (section 2.3) for obtaining matched observations. Although the totally different field of view among SFMR (looking downward from aircraft to the sea surface), TA radar (sampled from upward looking bins from aircraft altitude up to 3 km) and LF radar (sampled from bins 7 km ahead the aircraft and 10 azimuth degrees averaging from left to right of the aircraft track), it is believed that TA data is more comparable with SFMR because both of their data samples are taken from the vertical column of rain and the vertical path-integrated rain rate might be very different with the horizontal averaging rain rate. So for simplicity, we focus only on SFMR minus TA as the error of SFMR rain estimate in the following section of error analysis.

2.5 Error Analysis

To improve our understanding of how the error distribution is related to some hurricane parameters of interest, this section is devoted to investigate the rain type dependence, wind speed dependence, and radial distance dependence of errors.

2.5.1 Rain Type Dependence of Errors

It is still an open question how much variation in DSD may occur in hurricanes and whether there is any systematic difference between rain types. Here we use the results of section 2.4 to investigate this question for our database.

As noted in section 2.4, there is a different regression result for stratiform and convective samples. Fig. 2.6 gives PDFs and CDFs of SFMR rain rate errors (SFMR minus TA) for these two subsets. The standard deviation is 5.7 mm/hr (3.6 mm/hr) for convective (stratiform) rain, indicating relatively greater variation of DSD in convective regimes. The PDF of errors for stratiform samples peaks at 3 mm/hr, while the PDF for convective samples has two peaks, one is at –1 mm/hr, another is at +4 mm/hr. This also shows that the DSD in convective regions varies more than that in stratiform regions and a fixed K-R relation produces errors with both positive and negative values.

Although the effect of DSD variation on K-R relation can be seen clearly within convective regions, the mean error in convective rain (5.32 mm/hr) is only slightly larger than that in stratiform rain (4.48 mm/hr), a result showing that there is only a weak dependence of the K-R relation on rain type or DSD on average. This fact verifies that a separation of the K-R relation for different rain types would not produce a significant difference on the SFMR rain estimate.

Although we see from the regression for all samples that there is no error dependence on rain intensity, the SFMR error as a function of TA radar rain rate is investigated for stratiform and convective samples respectively (Fig. 2.7). Again, only a very weak dependence is found from Fig. 2.7, that is, SFMR error for stratiform

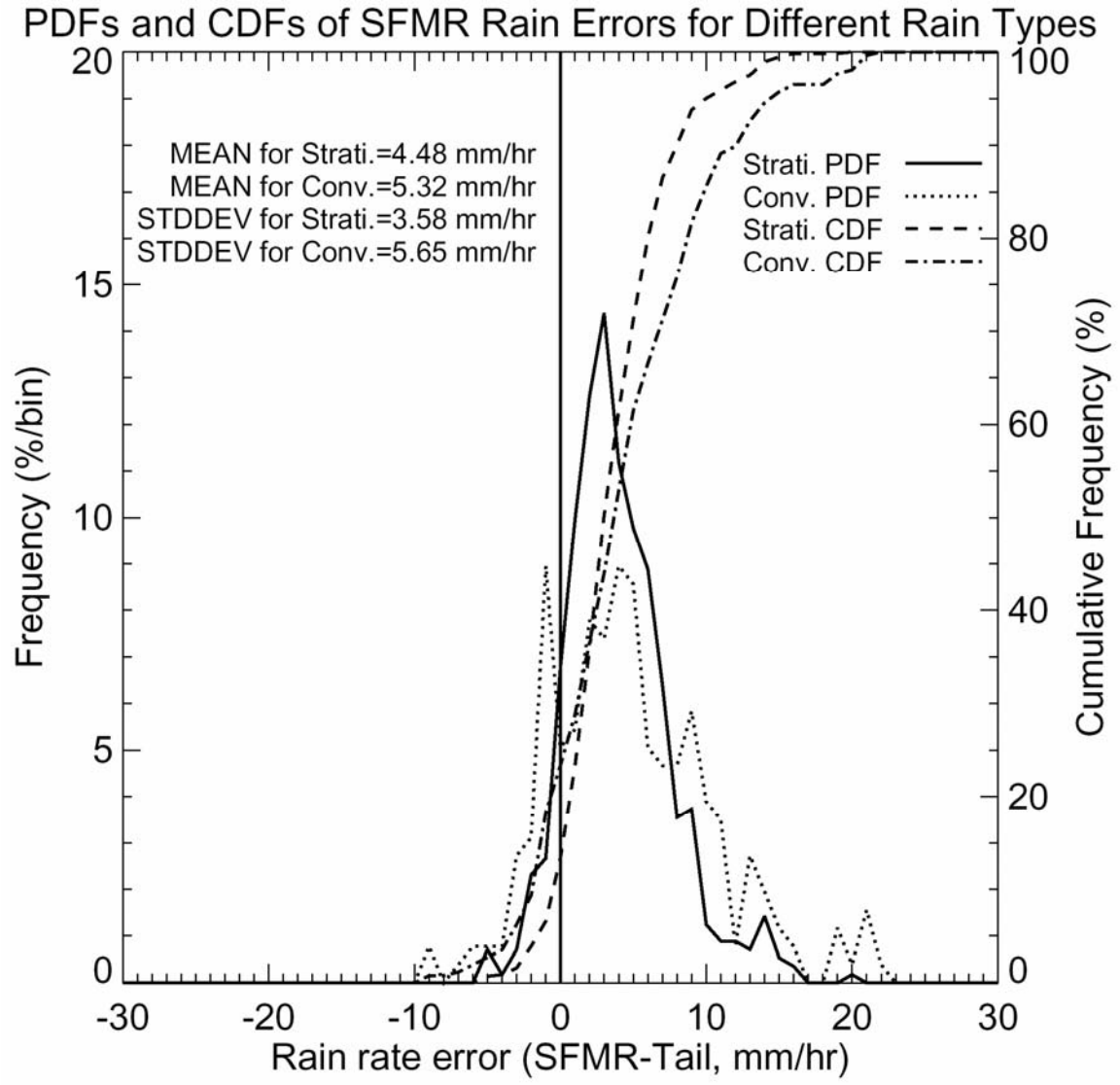

Figure 2.6. Probability density functions (PDF) of SFMR rain rate errors (SFMR – TA) for stratiform samples (solid line) and convective samples (dot line) and cumulative density function (CDF) of the SFMR rain rate errors for stratiform samples (solid line) and convective samples (dash dot line). Mean errors and standard deviations for these two sample subsets are indicated in the upper left corner of the figure.

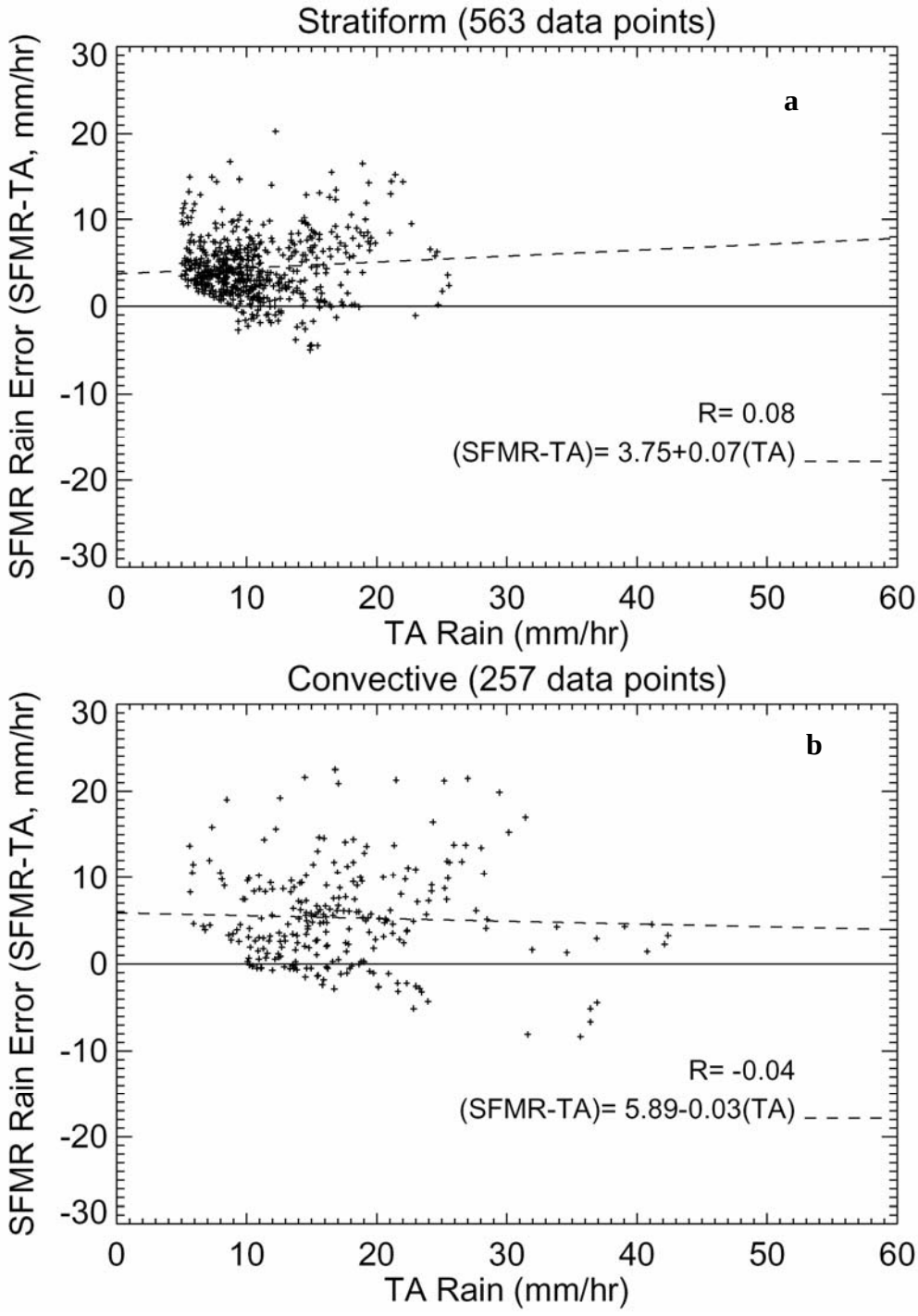

Figure 2.7. SFMR rain rate error relative to TA radar rain rate plotted as a function of TA rain rate (mm/hr) for (a) stratiform samples; (b) convective samples. Linear regressions (dash lines) and correlation coefficients (R) are indicated.

precipitation increases slightly with rain rate, but the reverse is the case for convective precipitation.

2.5.2 Wind Speed Dependence of Errors

The SFMR can estimate surface wind as well. Rain rate and wind speed are retrieved at the same time from the SFMR inversion algorithm, and Uhlhorn and Black (2003) reported an overall bias of 2~3 m/s of SFMR wind estimates relative to GPS 10-m winds. Although it was shown that this bias is independent on the magnitude of wind speed, we ask whether this kind of independence exists for the SFMR rain error as well. SFMR rain errors, again defined here as SFMR minus TA, are plotted as a function of SFMR wind speed in Fig. 2.8 for stratiform and convective separately. Here the SFMR wind speed is recalculated after the b-coefficient correction because SFMR wind retrieval depends on rain retrieval. A weak increase is seen in the SFMR's overestimation with increased SFMR surface wind for both rain types. The correlation coefficients are 0.25 for 563 stratiform samples and 0.24 for 257 convective samples respectively. Because SFMR wind is retrieved by relating it to the excess emissivity of wind-driven sea relative to specular emissivity of tropical ocean, it is highly possible that a wind-driven ocean produces more foam and spray that tends to increase the rain attenuation coefficient K compared to specular ocean conditions. From the regressions in Fig. 2.8, this wind effect tends to influence convective regions more than stratiform regions, the difference may not be significant.

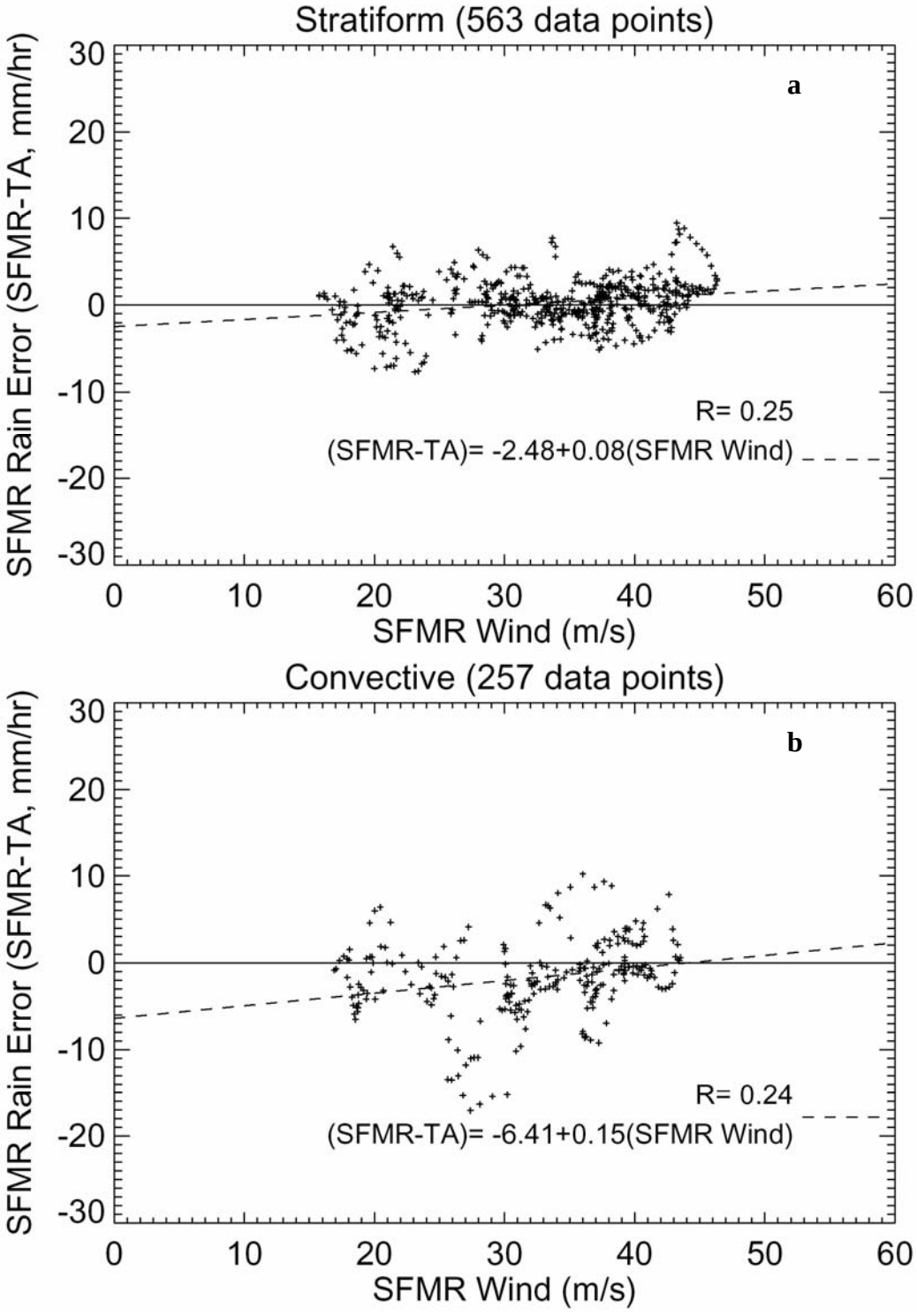

Figure 2.8. SFMR rain rate error relative to TA radar rain rate plotted as a function of SFMR wind speed (m/s) for (a) stratiform samples; (b) convective samples. Linear regressions (dash lines) and correlation coefficients (R) are indicated.

2.5.3 Radial Dependence of Errors

Rainfall, wind speed, and temperature in a hurricane are generally a function of radial distance r from the center. To find out the radial dependence of SFMR errors, the data have been analyzed according to their normalized radial distance, defined as r divided by the radius of maximum wind r_0. Hurricane spline fit storm track data fromaircraft observations (Neal M. Dorst, personal communication) is used to get r for each sample. For each radial tranverse, r_0 is identified from the SFMR data. A mean of these r0 for each storm is used to normalize r.

Fig. 2.9 plots the SFMR error as a function of normalized radial distance. All data used in this study were sampled within r/r_0 = 4. A decrease is obvious in SFMR error with increased distance from the storm center for both precipitation types. The correlation coefficients are 0.46 and 0.50, respectively. The similarity between correlation coefficients in Fig. 2.8 and Fig. 2.9 suggests that 1) there is no important difference of the error dependences for different rain types; 2) and the radial dependence of SFMR error may simply reflect the wind error. The temperature dependence on radius was also considered. Although the SFMR wind speed retrieval is not sensitive to sea surface temperature as tested by Uhlhorn and Black (2003), the rain retrieval does depend on the average air temperature in the SFMR illuminated volume (from aircraft altitude down to sea surface) because the temperature dependence of K-R relationship (Olsen et al. 1978). But the flight level temperature in our data set in most of the rain regions varies less than $1 \sim 2°C$, which produces a 2% rain rate error. So we can rule out the effect of temperature variation as a significant factor.

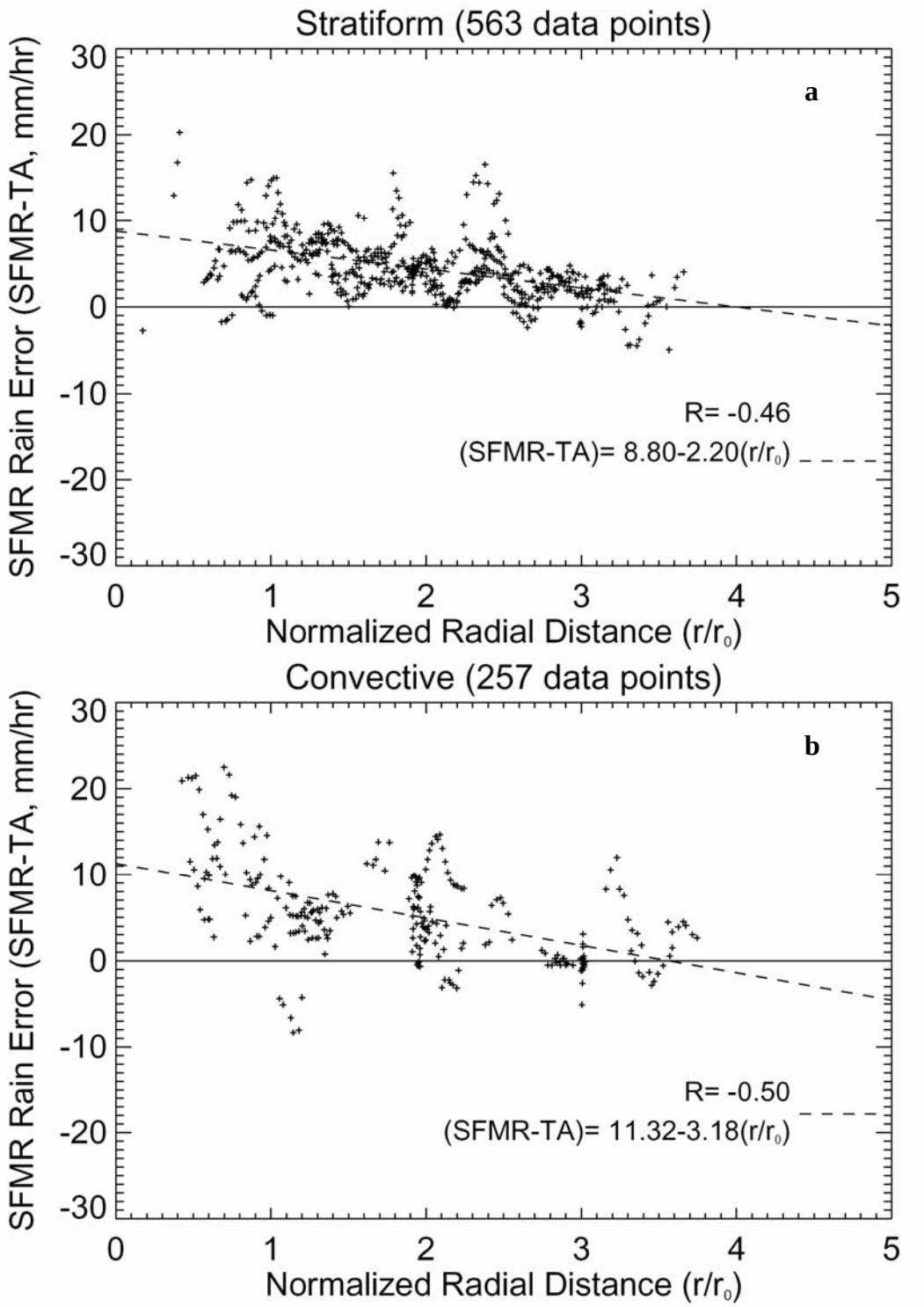

Figure 2.9. SFMR rain rate error relative to TA radar rain rate plotted as a function of normalized radial distance (r / r_0) for (a) stratiform samples; (b) convective samples. Linear regressions (dash lines) and correlation coefficients (R) are indicated.

2.6 Discussion

This chapter compares SFMR rain rates with radar measurements in a scheme for avoiding some limitations of airborne radar observations. In this scheme, the radar rain rate approximately corresponds to an average rain rate at 2 (or 1.5)~3 km altitude (the aircraft altitude can be 2 or 1.5 km), while SFMR corresponds to a path-integrated rain rate from 2 (or 1.5) km to the sea surface. As mentioned at the end of section 2.4, here we still only talk about the TA radar. The data sampling scheme of LF is similar to that of TA. Since in nature, the rain rate profile could be constant or increase downward or decrease downward in the lowest 3 km, it can be partially responsible for the discrepancies of SFMR estimates relative to radar. Although it is still open to debate (Zipser and Lutz 1994; Szoke and Zipser 1986; Steiner et al. 1995; Yuter and Houze 1995b; Heymsfield et al 2000), the shape of the vertical radar reflectivity profile in hurricanes has been investigated by some recent studies at the advent of TRMM. Ferreira et al. (2001) gave TRMM PR reflectivity profiles for the purpose of testing TRMM rainfall algorithms using two hurricane cases: Bonnie (1998) and Bret (1999). They showed the shape of PR standard algorithm 2A25 radar reflectivity profile in these two storms in stratiform and convective regions. From the mean profiles for Bonnie (see their Fig. 4a and Fig. 5a), it is obvious that the reflectivity increases from 3 km down to 1.5 km by 1 dB in stratiform rain and by 1~2 dB in convective rain. For Bret case, their Fig. 14 showed a 0 dBZ increase in stratiform regions and a 3 dBZ increase in convective regions. Combined those results, a 1~2 dBZ increasing from 3 km to 1.5 km was given by Ferreira et al (2001) on average. Their results are consistent with the Cecil et al. (2002) climatology from a 1-yr TRMM hurricane database (see their Fig. 3), and the

Heymsfield et al. (2000) EDOP mean reflectivity profiles for two Bonnie passes (see their Fig. 9 (b)). In the 820 samples used in this study, the mean LF and TA reflectivity is around 40 dBZ. By applying the Z-R relationship in (2.3), 1~2 dBZ reflectivity error at 40 dBZ corresponds to a rain error of 2.5~5.5 mm/hr. If we assume the slope of the vertical radar reflectivity profile in the lowest 3 km is as same as the Ferreira et al. (2001) result, that is, a 1~2 dBZ reflectivity increase for each 1.5 km altitude decrease all the way down to surface, then it is reasonable that the rain rate increasing from 2 (or 1.5)~3 km averaging to 0 ~ 2 (or 1.5) km averaging would be as same as this 2.5~5.5 mm/hr difference between 3 and 1.5 km. In Fig. 2.6, the mean SFMR error of 4.48 mm/hr for stratiform and 5.32 mm/hr in convective rain would be mostly canceled out if we take this altitude discrepancy between SFMR and radar samples into account, leaving an error within ± 2 mm/hr. An uncertainty of the vertical radar reflectivity in the lowest 1.5 km is not counted in above analysis. Typically, because of the ground clutter contamination, PR and ground-based radar could not detect the lowest 1-2 km of storms. A climatology of the lowest part of the vertical radar reflectivity for hurricanes could be done by using data from high quality radar with high vertical resolution, such as EDOP (assuming that the attenuation problem of EDOP can be dealt with accurately).

The near independence of the K-R relation on precipitation types in hurricanes shown in this study is consistent with Jorgensen and Willis's (1982) result on the independence of Z-R relation on rain types. Although the K-R relation used in the SFMR algorithm has a rain rate-dependent "a" coefficient, it doesn't account all effects of different rain types. So the overall independence on rain types for both Z-R and K-R relations must imply something about DSD in hurricanes. With the verification from two

independent studies, one may conclude that the variation of DSD in hurricanes is relatively small, on average, between convective and stratiform rain types.

The variation of DSD and Z-R and K-R relations in different rain types has been studied extensively for many kinds of precipitation systems other than hurricanes. Stout and Mueller (1968) summarized that in radar rainfall estimates there are differences on the order of 150% that can be attributed to different types of rain or different synoptic conditions. Delrieu et al. (2000) presented the K-R relation variations among "widespread," "thunderstorm," and the intensive long-lasting autumn rain events in Cevennes in France. Compared with above studies, the conclusion of the near-independence of DSD on rain types in hurricanes in this study is paradoxical. But this apparent discrepancy could be explained by considering the special hurricane precipitation environment. By using airborne Doppler radar observations in Hurricane Alicia, Marks and Houze (1987) found that the precipitation particles advected from the upper levels of the eyewall by the radial flow are carried azimuthally as many as one-and-a-half times around the storm by the strong tangential flow of the vortex before they reach the melting level. Houze et al. (1992) called hurricane as a giant "mixmaster" that stirs and tends to homogenize the precipitation region lying just outside the eyewall. It is probable that the variation of DSD between convective and stratiform rain in hurricanes is minimized by the large horizontal wind, which is distinctly different from other rain systems. It is also extensively verified that the convective intensity in hurricanes and other tropical oceanic features is generally modest compared with precipitation features over continents by Cecil et al. (2002) and Jorgensen et al. (1985). In these studies, even in the convective cases, the radar reflectivity profiles above the freezing level decrease

rapidly with height and the updraft magnitudes are far less than that in continental convection. Therefore, the characteristics of convective rain in hurricanes may be somewhat similar to those in stratiform rain.

2.7 Conclusion

The passive microwave radiometer is a useful tool for measurement of path-integrated rain rates in hurricanes. The "path integrated" means that the SFMR senses the microwave emissions, and therefore brightness temperatures, mainly from the whole rain column from the aircraft to the sea surface. The instrumentation of SFMR has an additional advantage that it will not saturate until a very high rain rate, unlike other radiometers with higher frequencies. The SFMR retrieved rain rates are well correlated with airborne radar rainfall measurements. After checking the algorithm carefully, the insensitivity of SFMR rain relative to radar observations has been removed by a b-coefficient correction. The SFMR provides independent estimates of rain rates at a horizontal resolution of ~ 10 s (1.5 km) along the flight track. The SFMR rainfall is another important measurement in hurricanes for operational applications.

An overall high bias (~ 5 mm/hr) of the SFMR rain rate estimates relative to radar was found. We speculated that this may be potentially explained by the comparison scheme for avoiding the limitations of the radar observations. The radar "truth" used for comparing with SFMR path-integrated rain rate between 0~2 (or 0~1.5) km is relative to a 2~3 (1.5~3) km average rain value. The elevation difference of the data may cause an up to 3~5 mm/hr bias if the true slope of vertical radar reflectivity is 1~2 dBZ per 1.5 km increasing downward at the lowest 3 km (as in Ferreira et al. 2001). But one should be

cautious since the radar reflectivity profile in the lowest 1.5 km is unknown for most radars because of ground clutter. Another factor to explain the SFMR high bias is the sensitivity of SFMR estimates to fractional coverage of the sea surface foam and spray. This is found by examining the dependence of SFMR rain error relative to radar on wind speed and normalized radial distance to the storm center.

Near-independence of SFMR rain errors on rain types is found. It is inferred that the K-R relation in hurricanes is similar for different precipitation types. Combined with Jorgensen and Willis's (1982) result of the independence of the Z-R relation on different rain types in hurricanes, this result supports the conclusion that the variation of DSD in hurricanes is small relative to other precipitation systems. This could be explained by the Houze et al. (1992) "mixmaster" idea citing the homogenizing effect of the strong tangential wind. This is also consistent with previous radar, lightning, updraft magnitude, and radiometer studies (Cecil and Zipser 2002; Molinari et al. 1996; Black et al. 1996; Szoke et al 1986; and Jorgensen et al. 1985). These studies showed that the convective intensity in hurricanes is modest, and that its difference from stratiform rain is minimized compared with continental storms.

2.8 Appendix: Calibration of LF and TA Radar

The calibration of TA and LF radar can shift as a result of repairs, upgrades, and other factors. The general statement of the calibration error of TA and LF is as great as 5~6 dB (Oury et al. 1999, Marks et al. 1993), but it varies year by year due to major updates and repairs at the beginning of each hurricane season. As concluded by Atlas (2002), "After 56 years research in radar meteorology, we have still failed to find a

reliable and universally applicable method of radar calibration." However, for individual applications, some successful calibration methods were developed. Marks et al. (1993) presented a method to calibrate LF radar by using the drop size distribution (DSD) measurement on aircraft during Hurricane Anita (1977). An 8.2 dB underestimate was found for LF radar during the 1977 mission season.

Another way to determine the radar calibration error is to use a well-calibrated radar for comparison. The Tropical Rainfall Measurement Mission (TRMM) Precipitation Radar (PR) data have been used to calibrate ground-base radar data (Anagnostou et al. 2000; Bolen and Chandrasekar 2000; Schumacher and Houze 2000) because of the remarkable stability of PR. The NASA ER-2 Doppler radar (EDOP) has very stable characteristics, and it has been compared with the PR. The EDOP is an X-band (9.6 GHz) Doppler radar with fixed nadir and forward pointing beams with a beam width of $2.9°$. It flies on the NASA ER-2 aircraft at 20 km altitude and can map out the reflectivities and Doppler winds in the vertical plane along the aircraft path. A detailed description of the EDOP instrument can be found in Heymsfield et al. (1996). During the joint NASA/NOAA aircraft-based field programs into tropical cyclones in 1998 and 2001, a large volume of coordinated EDOP, TA and LF radar data were collected. Hurricane Bonnie (1998) and Humberto (2001) data are dealt with separately to find preliminary calibration estimates.

Two steps are involved in the preliminary TA and LF calibration estimate. Because both EDOP and TA obtain data in a vertical plane, we compare TA with EDOP in the first step by using along-track vertical cross section data. The second step is to obtain LF calibration estimate by comparing with corrected TA data. In the EDOP-TA comparison,

reflectivity data above 2 km are used to minimize the attenuation effect for EDOP and to eliminate the “French Antenna” problem of TA (section 2.3.2). During Bonnie flights, although there is no exactly matched flight pass between ER-2 and N43RF aircraft, a long time period of data sample (e.g. totally 5-hr flight for EDOP and 6-hr flight for TA) is recorded by both EDOP and TA during Aug. 24 & 26, 1998. By assuming the whole storm was sampled comparably by both radars in this long period flights, the histograms of EDOP and TA reflectivity in the along track vertical cross section above 2 km are compared. A +6 dB offset is found for TA reflectivity during Bonnie 1998. Fig. 2.10 gives the comparison of probability density functions (PDFs) and cumulative density function (CDFs) of the EDOP reflectivity and TA corrected reflectivity (+6.0 dB). Except for the range of 0-6 dB, which is in a no-rain region, a good agreement can be seen between EDOP and corrected TA data. The error analysis given in Table 2.5 shows that this +6.0 dBZ correction on TA reflectivity produces an error of $\pm 1 \sim 2$ dB by comparing with EDOP CDFs. During Humberto (2001) flights, a nearly exactly matched leg is found around 21:40 UTC on Sept. 23. Comparing the histograms of EDOP and TA reflectivity during this leg, a +4.5 dB offset is put on TA data for a preliminary calibration estimate. Fig. 2.11 shows the comparison of PDFs and CDFs of EDOP and TA dBZs during this leg after shifting +4.5 dB for TA. There is a good agreement above 20 dBZ, but below that, the frequency difference may be caused by the small mismatch at the edge of this leg. The error analysis is also given in Table 2.5, showing an error within $\pm 1 \sim 2$ dB after calibration, which is sufficient for the analyses of this paper.

LF is calibrated by comparing the LF and TA along-track averaged dBZ values. The along-track averaged dBZ data is produced by using the scheme described in section

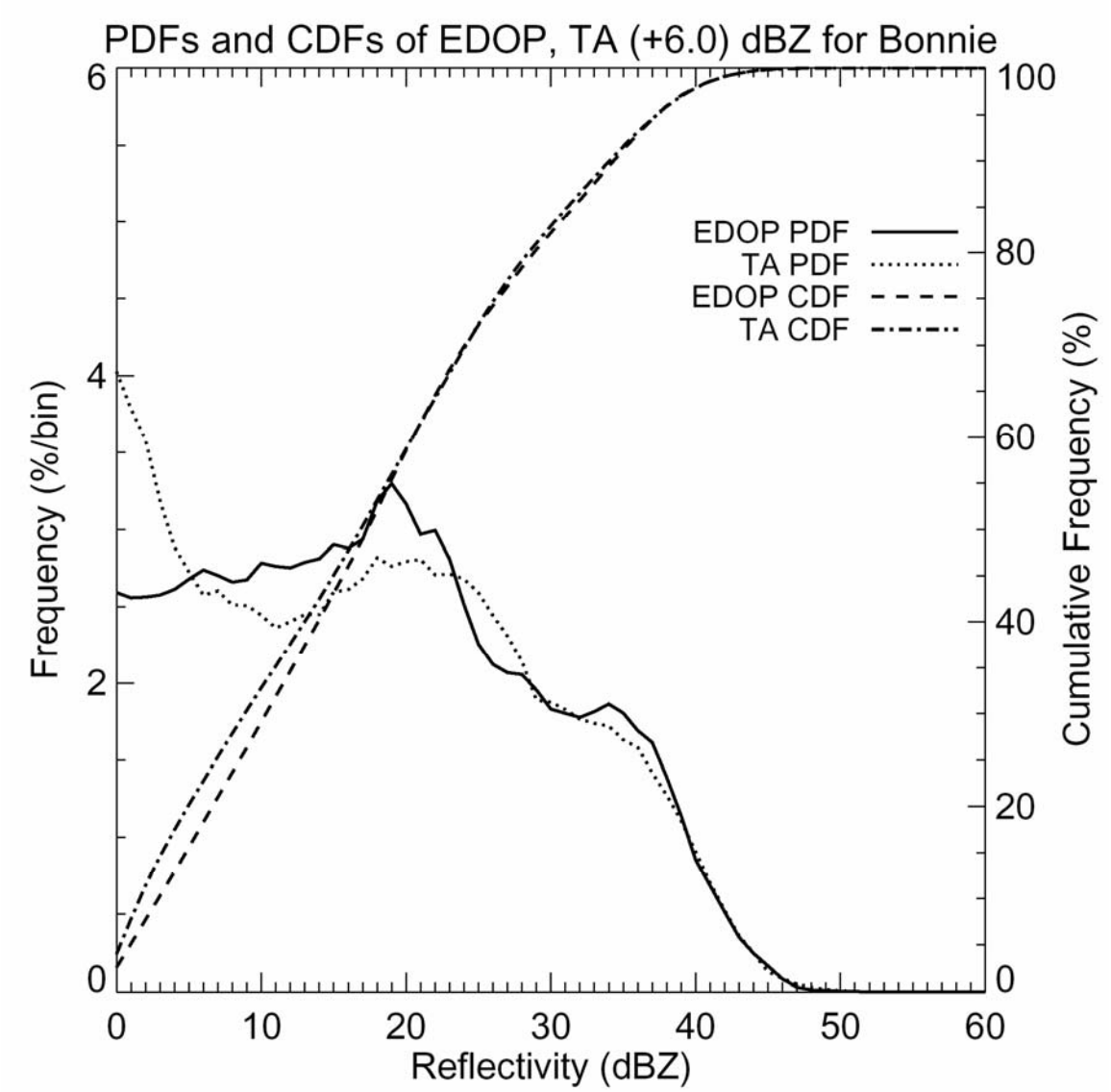

Figure 2.10. Probability density functions (PDFs) and cumulative density function (CDFs) of the EDOP reflectivity and TA corrected reflectivity (+6.0 dB) during Hurricane Bonnie flights during Aug. 24 and 26, 1998.

Table 2.5. Statistics of the bias of TA corrected reflectivity according to EDOP (EDOP-TA Corrected) at mean and selected percentile levels (in dB)

	Bonnie	Humberto
Mean	+0.73	+0.52
10%	+1.28	+0.99
30%	+1.47	+1.71
50%	+0.47	+0.64
70%	-0.08	-0.37
90%	+0.29	+0.43

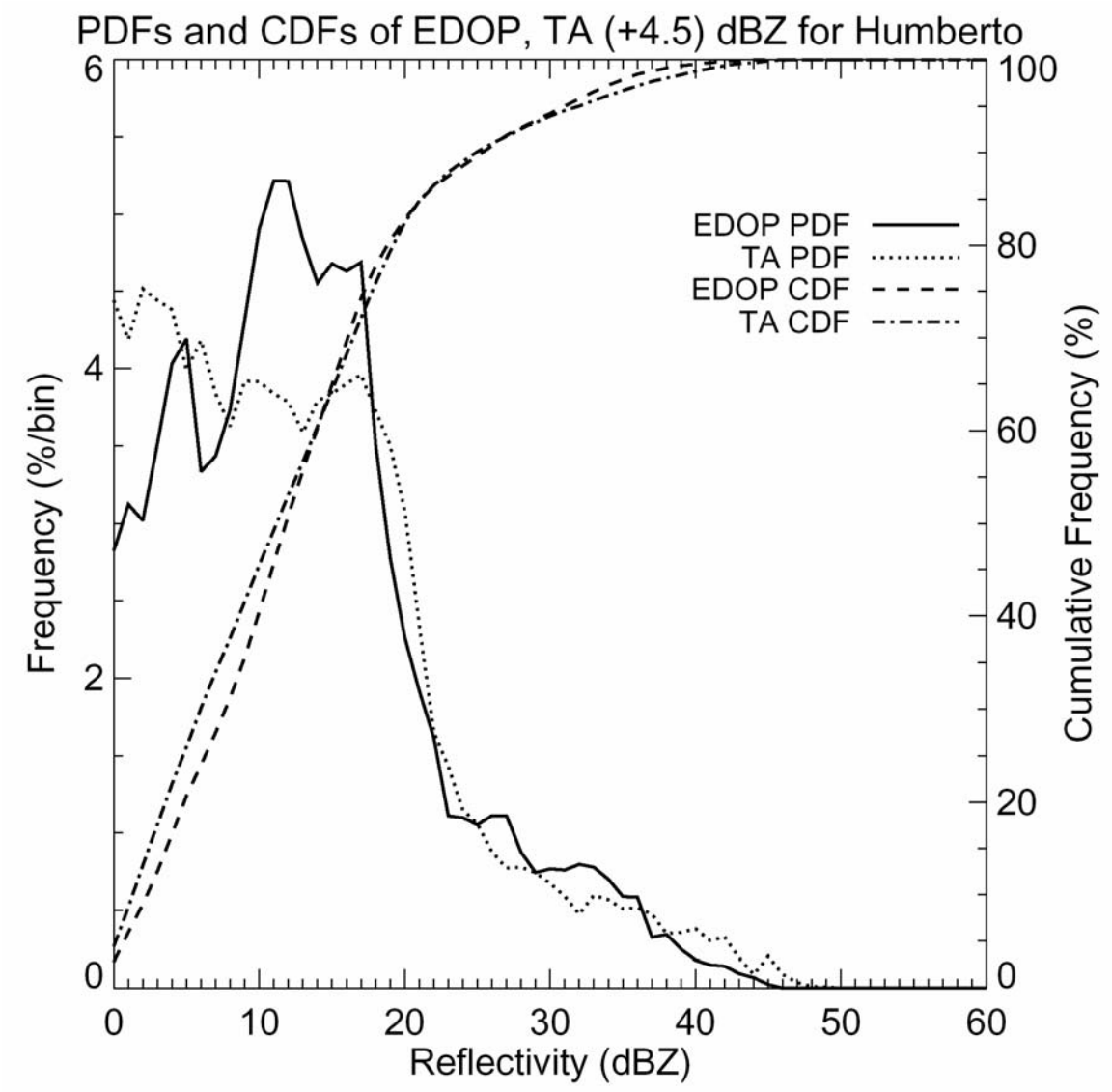

Figure 2.11. Probability density functions (PDFs) and cumulative density function (CDFs) of the EDOP reflectivity and TA corrected reflectivity (+4.5 dB) during one Hurricane Humberto flight leg around 21:40 UTC on Sept. 23, 2001.

2.3. No calibration error is found for LF during the Bonnie mission, while a +6.5 dB offset is found for the Humberto mission.